

This pdf file consists of figures containing photographs, and their captions,
scanned from:

**OCEANIC FAULTING AND HYDROTHERMAL CIRCULATION WITHIN THE
CRUSTAL SEQUENCE OF THE JOSEPHINE OPHIOLITE,
NORTHWEST CALIFORNIA AND SOUTHWEST OREGON, USA**

by

Robert J. Alexander, B.A., M.S.

Abstract of

A Dissertation

Submitted to the State University of New York at Albany

in Partial Fulfillment

of the Requirements for the Degree of

Doctor of Philosophy

College of Science and Mathematics

Department of Geological Sciences

1992

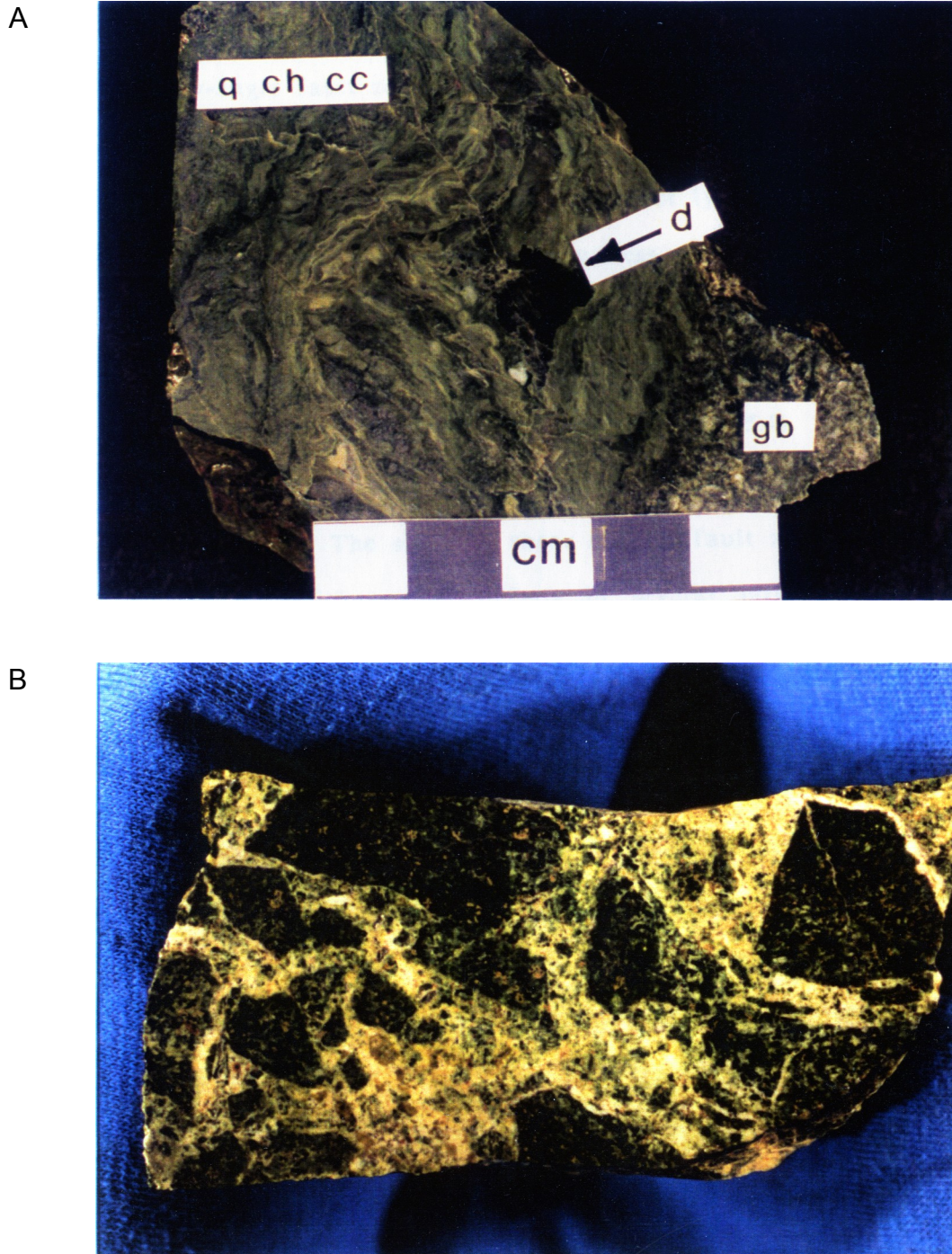
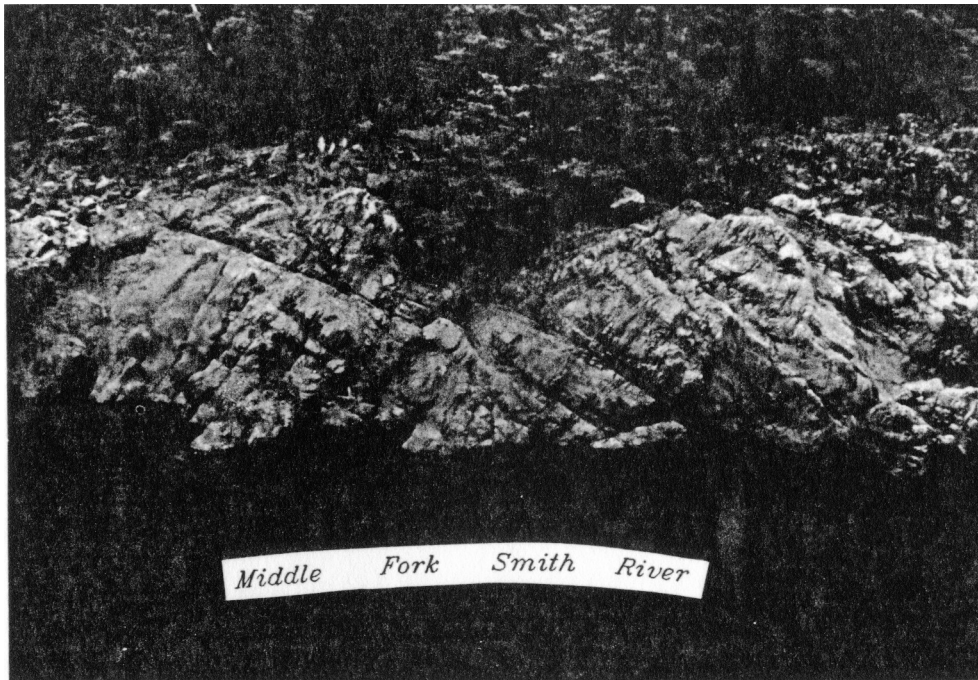


Figure 3.11 Photographs of fault rocks from the RH Mine area. (A) Ultracataclasite/ protomylonite with matrix of quartz (q), chlorite (ch), and calcite (cc) and localized highly altered porphyroclasts of diabase (d) and gabbro (gb). (B) Hydrothermally cemented breccia in footwall of main fault with clasts of ultramafic and mafic gabbro and cemented by different generations of epidote, prehnite, and local hematite.



Figure 4.2: Photographs of discontinuous dikes with stepped margins. Serial sawcuts (~3 cm apart) through a hand sample of a thin overlapping, en echelon dike with a "bridge" of wall rock between two segments (a) and lateral transition into a simple dike step (b). Note that the prehnite vein, which is crosscut by the overlapping dikes, has an apparent shear offset which is really due to bridge rotation.

5A



Outcrop Sketch at Big Bend

5B

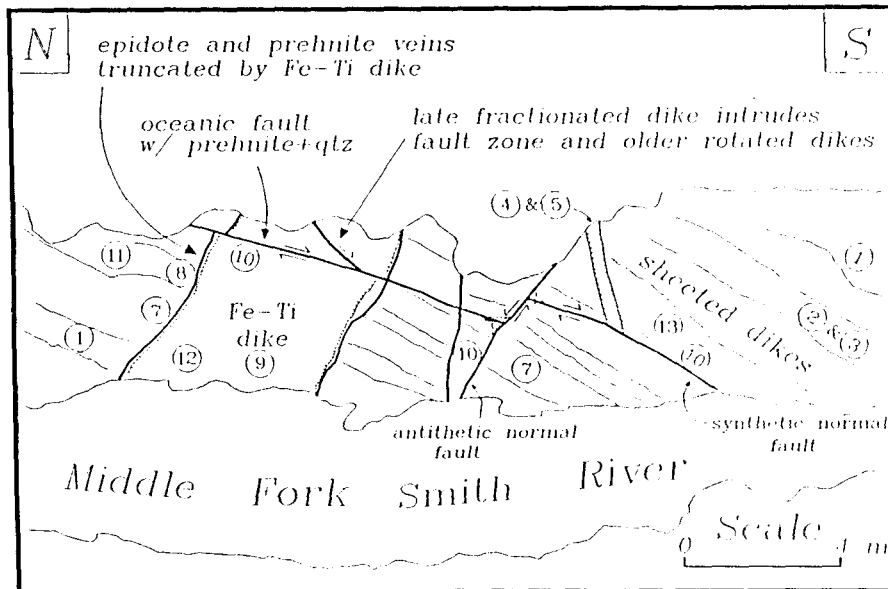


Figure 6.5 (A) Photograph of a water-polished exposure of the basal sheeted dyke complex which is in the core of a gently ($\sim 10^\circ$) southward-plunging syncline, so structures are in their original oceanic positions. (B) Line drawing of photograph showing locations of gabbro screens, older rotated sheeted dykes, hydrothermal veins, a thick Fe-Ti enriched dyke, and oceanic normal faults (synthetic and antithetic-dipping). Numbers correspond to events listed in figure 5c.

6A

6B

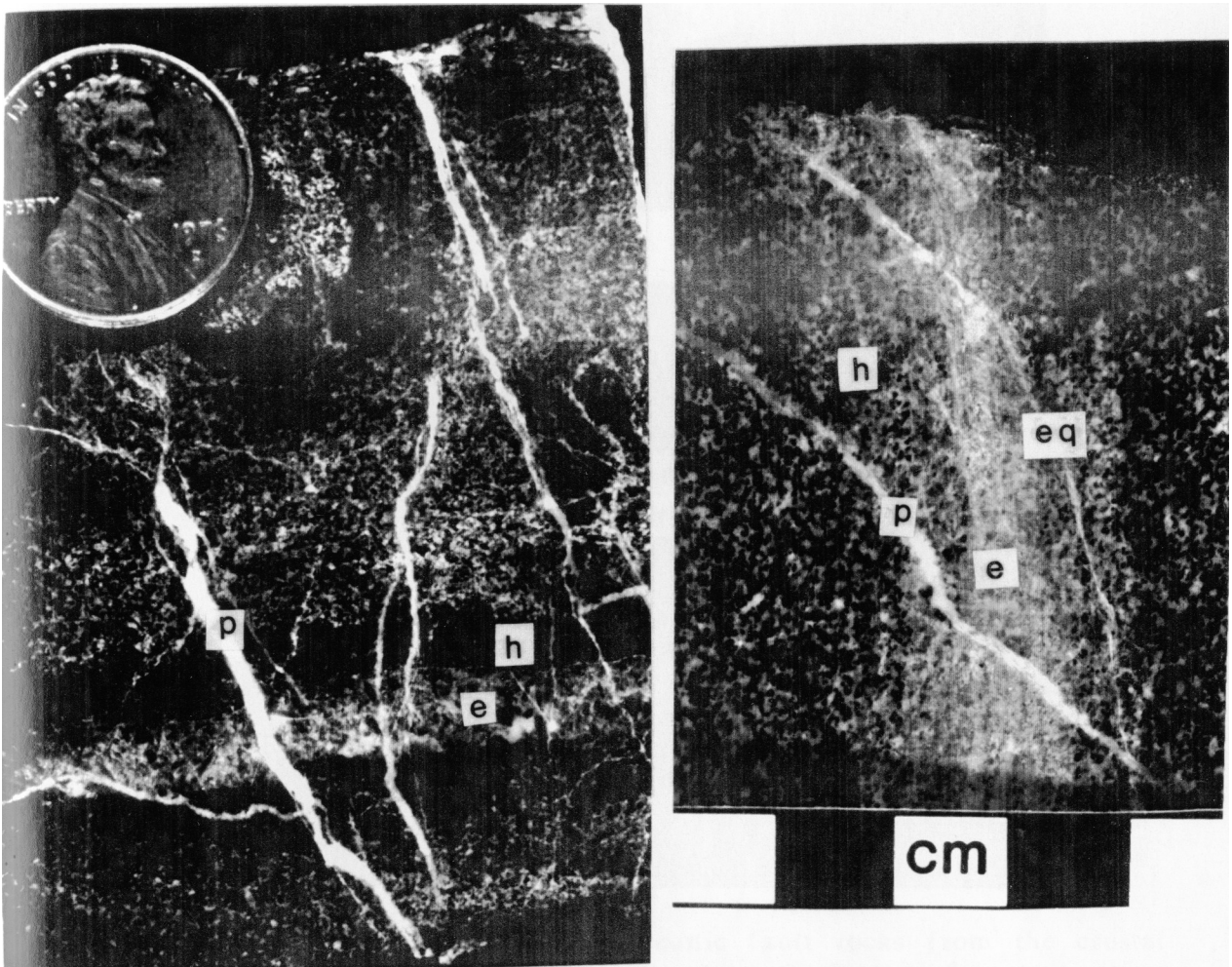


Figure 6.6 Photographs of fine-grained gabbros with several sets of hydrothermal veins showing consistent cross-cutting relationships and suggesting a drop in fluid temperature and/or a change in fluid composition with time. (A) Micro-gabbro with Fe-rich, zoned epidote vein (e) and darker actinolitic hornblende + magnetite halo (h) which is cross-cut by white prehnite veins (p). (B) Fine-grained gabbro with dark diffuse hornblende + magnetite vein (h) which is cross-cut by a wide epidote vein along a small fault (e), which is in turn cross-cut by an epidote + quartz vein (eq). Finally, all veins are cross-cut by a white prehnite vein (p).

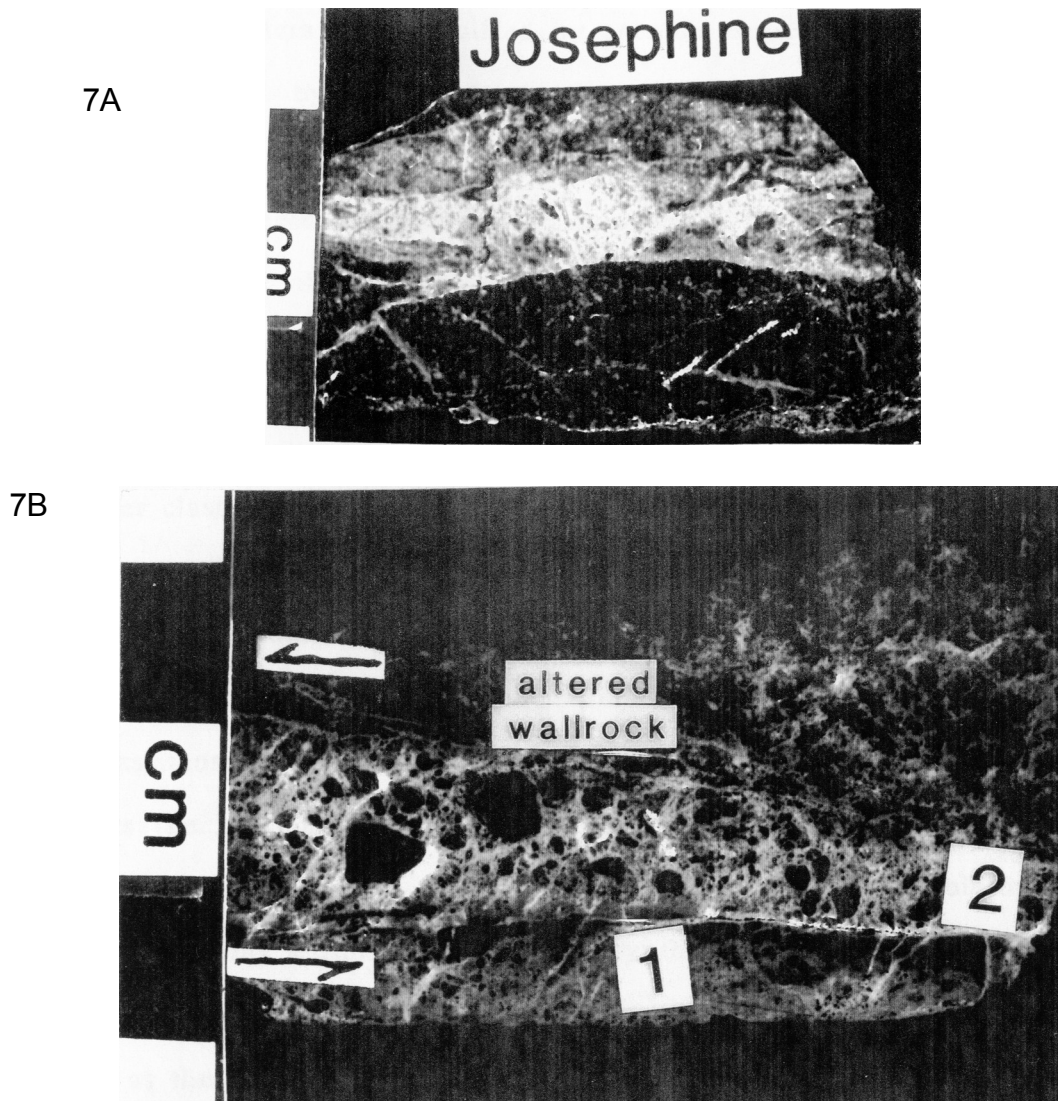
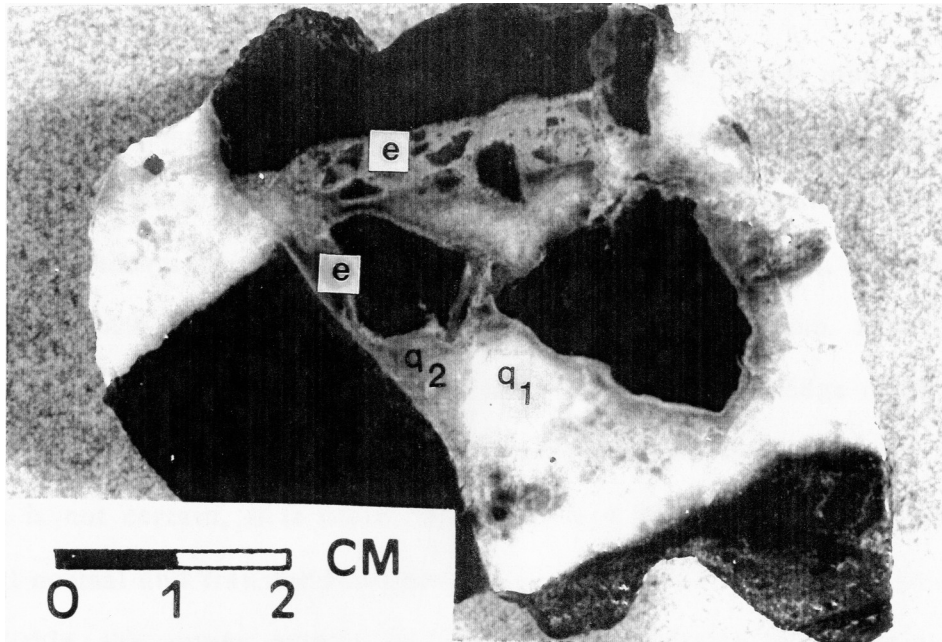


Figure 6.7 Photographs of brittle oceanic fault rocks from the crustal sequence of the Josephine ophiolite. Note extreme degree of metasomatism required by local complete pseudomorphic replacement of diabase fragments by hydrothermal minerals. Also note grain-size reduction and clast fragments set within fault gouge which is now recrystallized. Subseafloor hydrothermal minerals are predominantly restricted to the fault zones and adjacent fractured wall rocks, but do not extensively affect unfractured bedrock away from the faults. (A) Example of a cataclasite from the sheeted dyke complex cemented by at least two episodes of epidote, indicating multiple fault reactivation. The fault zone is approximately parallel to dyke margins. (B) Oceanic cataclasite with relict diabase clasts, cemented by quartz + prehnite, and cross-cut by an echelon tension vein array showing a left-lateral shear sense. Multiple episodes of movement and static recementation are evident in hand sample (1 and 2, on photo) and in thin section based on the presence of clasts of older cataclasite in fault zone, the contrast in grain-size and composition of different generations of cements, and the local presence of shear fractures in the cements.

8A



8B

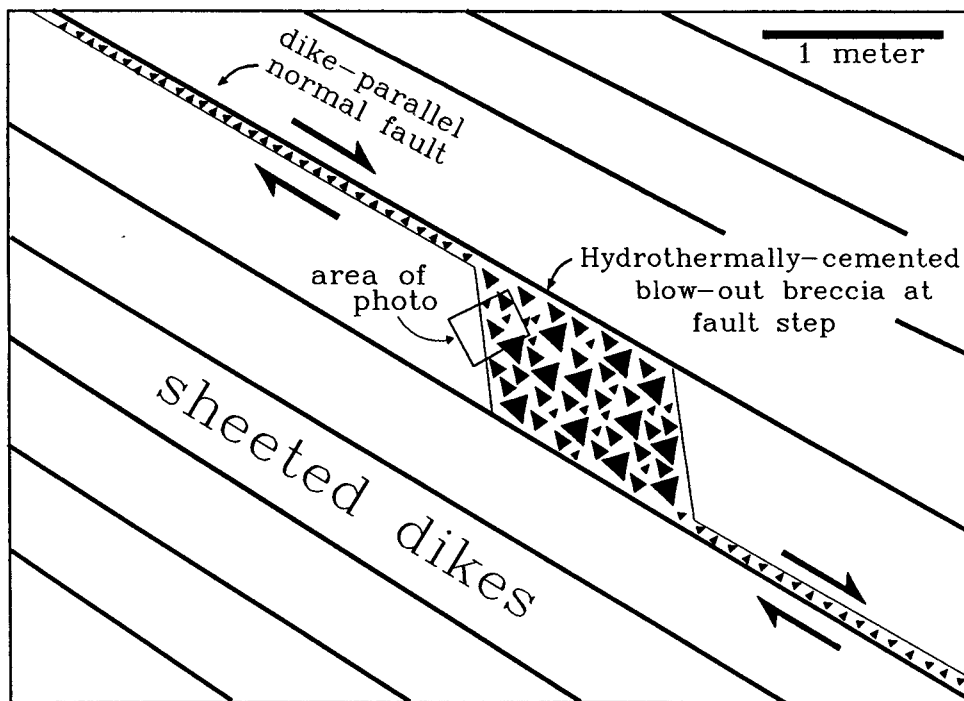


Figure 6.8 Photograph of a hydrothermally-cemented breccia and sketch of its outcrop setting within the sheeted dyke complex (Loc. 8, Fig. 6.1). (A) Angular diabase clasts (d) with typical discharge sulfides cemented with a thin rim of epidote (e) and then filled in with two generations of quartz, cloudy and clear (q_1 and q_2). All features are locally cross-cut by late hematite veins (not shown). (B) Sketch showing outcrop setting of the breccia along a small trans-tensional discontinuity along an oceanic normal fault which is parallel to sheeted dyke margins.

9B

9C

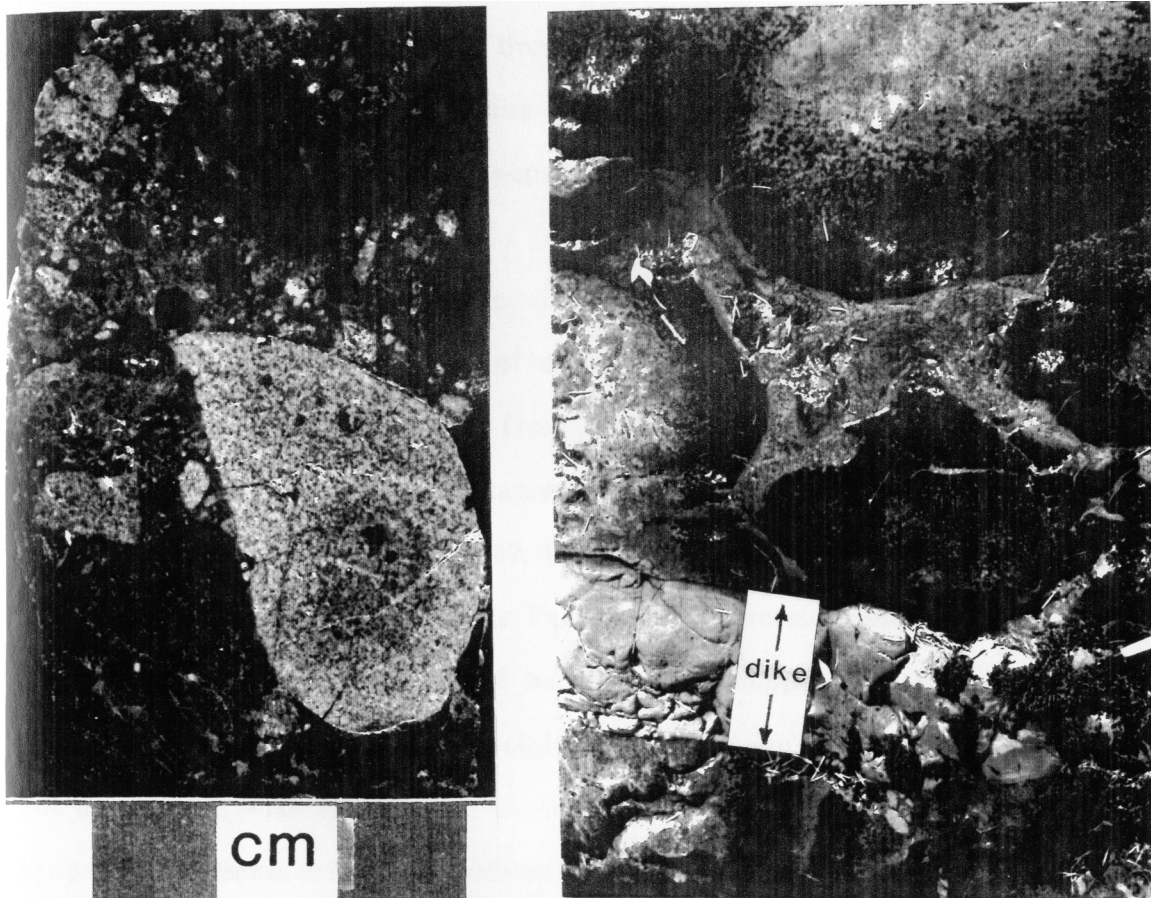


Figure 6.9 (cont.) Photographs of a heterolithic sedimentary talus breccia (B) and pillow basalt (C) which occur as screens within the sheeted dyke complex (Loc. 8, Fig. 6.1). Clast types in the breccia include, in decreasing abundances: diabase, basalt, silicified basalt, and hemipelagic chert. Matrix material is silicified hemipelagic and hyaloclastic(?) material which locally is pervasively mineralized with sulfides. Pillow screen shows variolitic primitive pillows and interpillow matrix which are cross-cut by a dyke which shows pure dilation. Composite diagram of upper crustal sequence shows geological setting of these and other types of "out-of-place" screens in the sheeted dyke complex (Fig. 6.15b).

10C

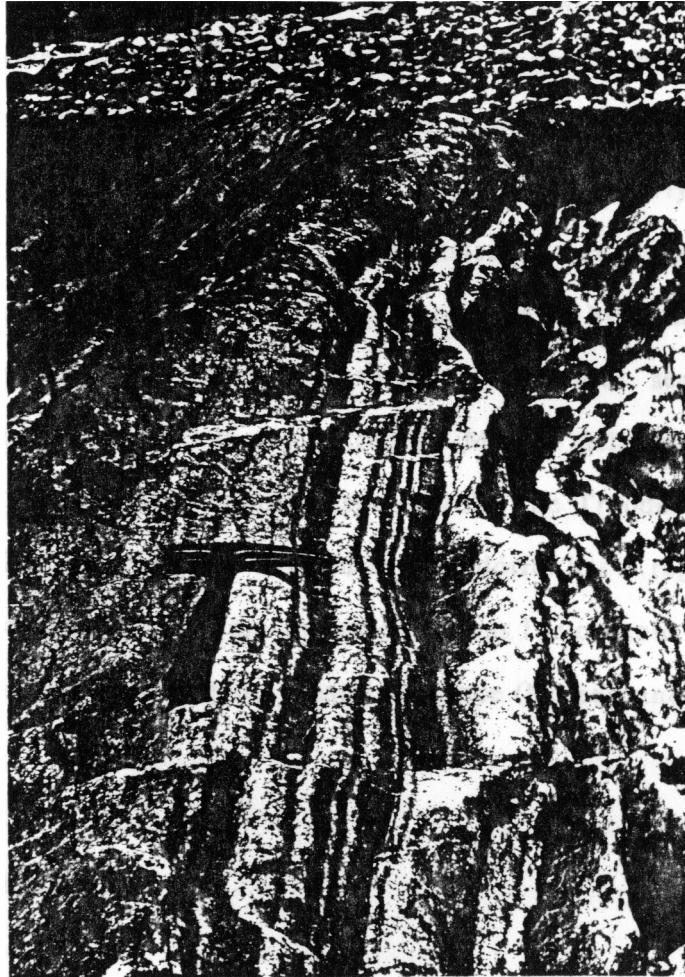


Figure 6.10 (cont.) (C) Photograph parallel to layering in cumulate gabbro showing small offsets along clinozoisite veins and also showing bend fold (i.e. "drag") of layering in the footwall of the fault zone.

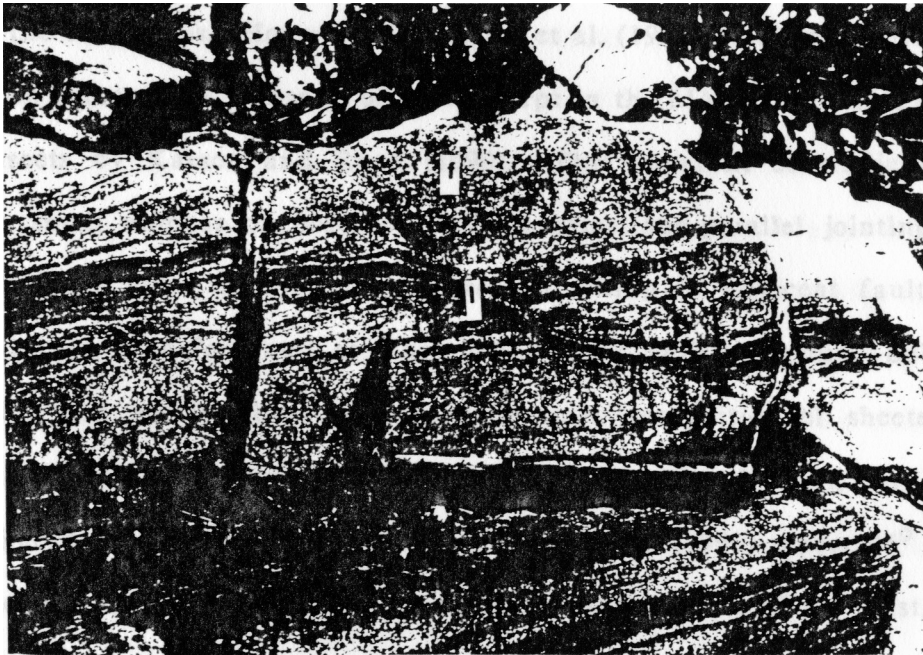


Figure 6.12 Photograph of layered gabbro with an outcrop scale listric normal fault (l) showing super-solidus slumping or high-temperature sub-solidus plastic deformation. Also, note the presence of several small-scale, regularly-spaced, planar fractures (f) in the hangingwall and footwall blocks which dip towards the right and may represent incipient brittle fracturing. Deformation must be oceanic in origin because the high temperature fabric is defined by igneous minerals. Hammer is 25 cm long for scale.

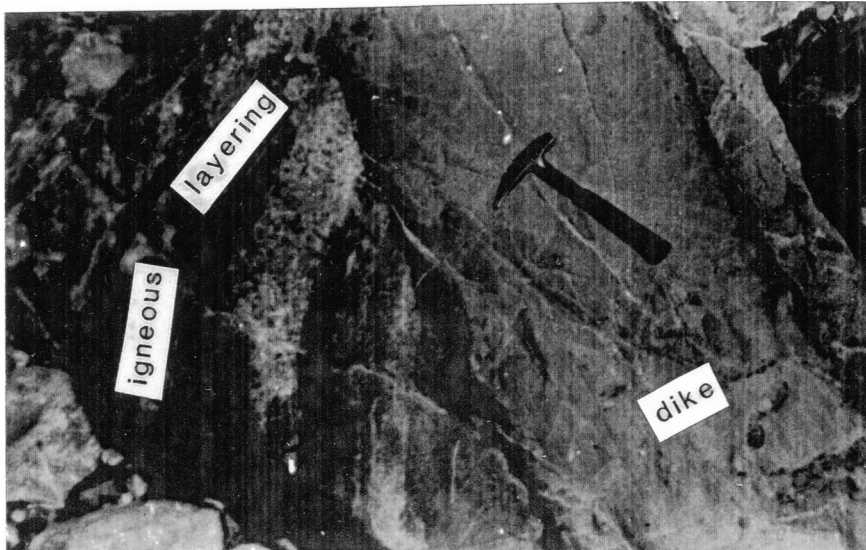


Figure 6.17 Photograph of a doubly-chilled dyke (d) which clearly cross-cuts older igneous layering in a coarse-grained gabbro at an oblique angle. If the layering was initially sub-horizontal and the dyke was intruded vertically, then this requires a considerable amount of tilting of the igneous layering ($\sim 40^\circ$) prior to intrusion of the dyke.

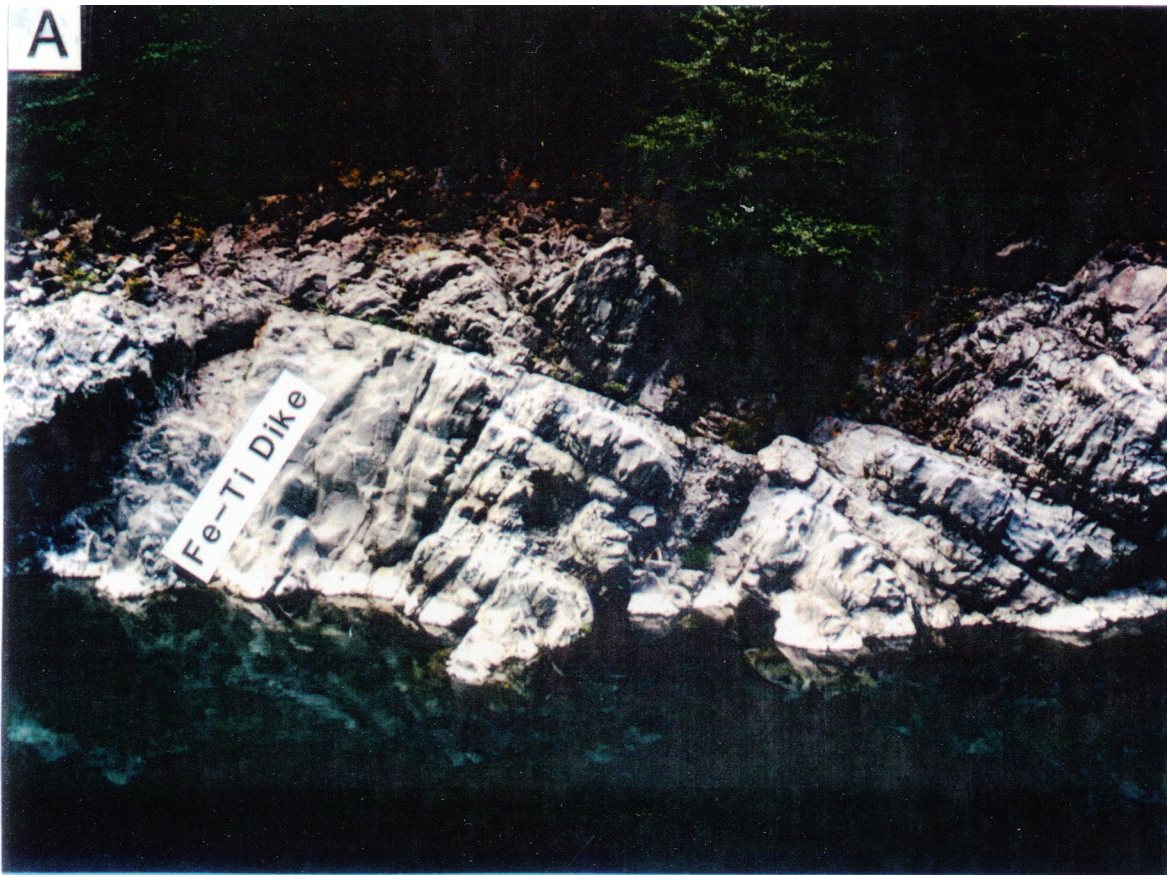


Figure 2 [a] Photograph of the water-polished outcrop of sheeted dike/gabbro transition zone. Tilted dikes dip to the right (south) and are crosscut by a thick subvertical dike in the left side of photograph. See text and Figures 4 and 6a.

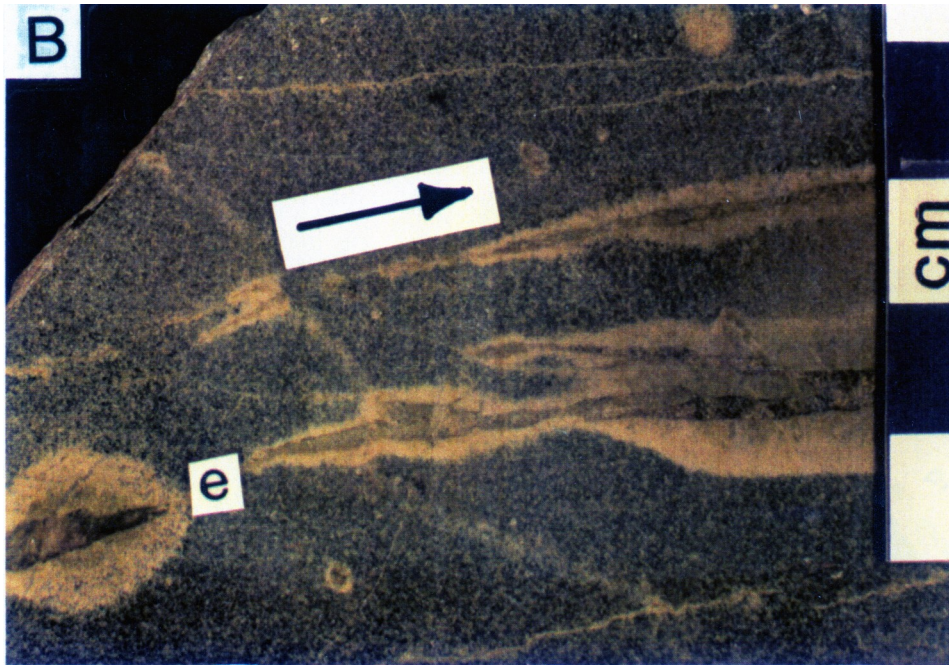


Figure 2 [b] Dike-parallel epidote (e) veins with epidosite alteration halos in diabase dike. Arrow is parallel to dike margin. Not from locality discussed in text.



Figure 2 [c] Dike-parallel epidote vein (R44, Table 3) in coarse diabase dike (right) crosscut by a very fine-grained dike (left). Epidote vein and both dikes are cross-cut by white prehnite veins.

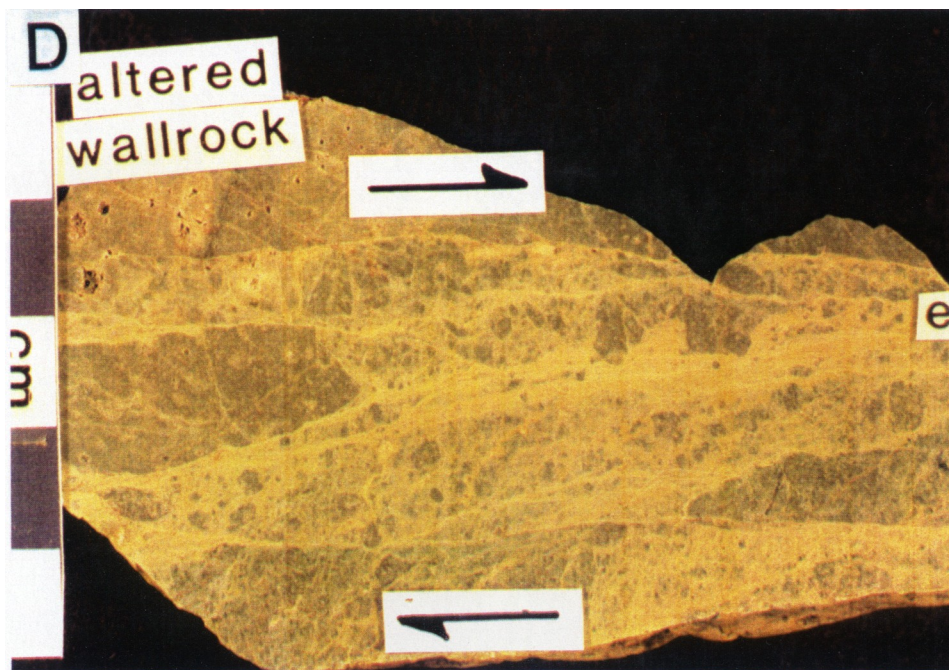


Figure 2 [d] Typical epidote (e) \pm quartz cemented dike-parallel cataclasite. Diabase clasts are altered to greenschist facies assemblage. Arrows indicate slip sense determined by offset wall rock markers, the geometry of secondary fractures (RM) and offset clasts.

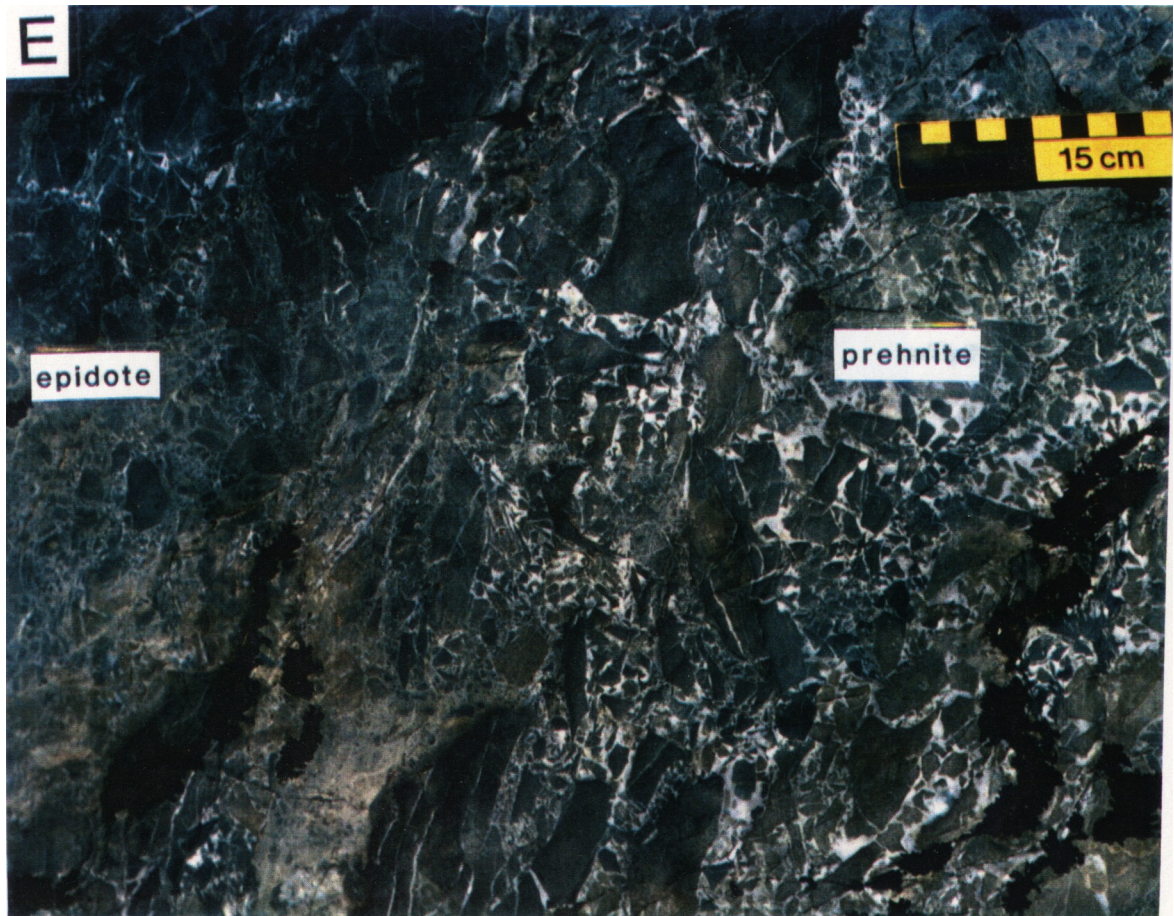


Figure 2 [e] Multiply-reactivated fault zone breccia at extensional step in a dike-parallel fault zone. Epidote + quartz cemented breccia (left) are locally crosscut brecciated by a later fault slip event and recemented by prehnite + quartz cement.

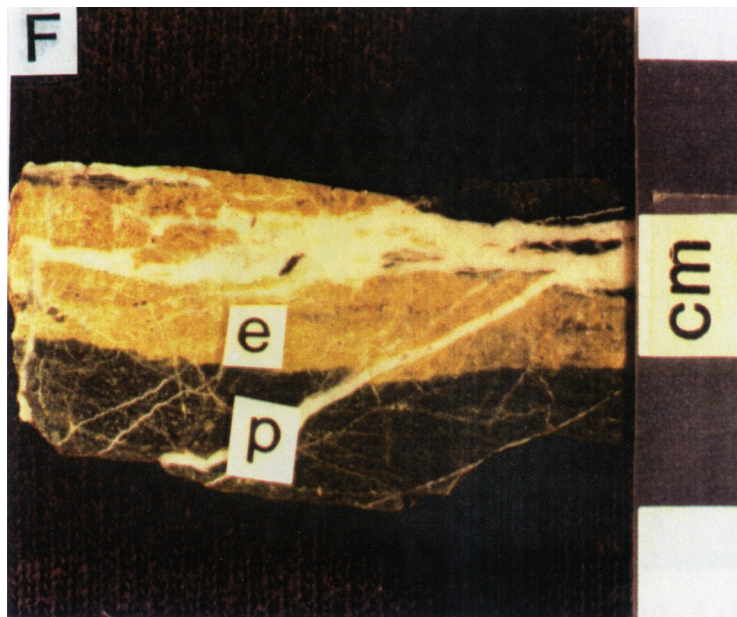


Figure 2 [f] Dike-parallel epidote vein (e) is cross-cut by a prehnite vein (88-15a, Table 3). Both veins are cross-cut by the thick subvertical dike shown in Figure 2g (event #9, Figures 6a and 6b).

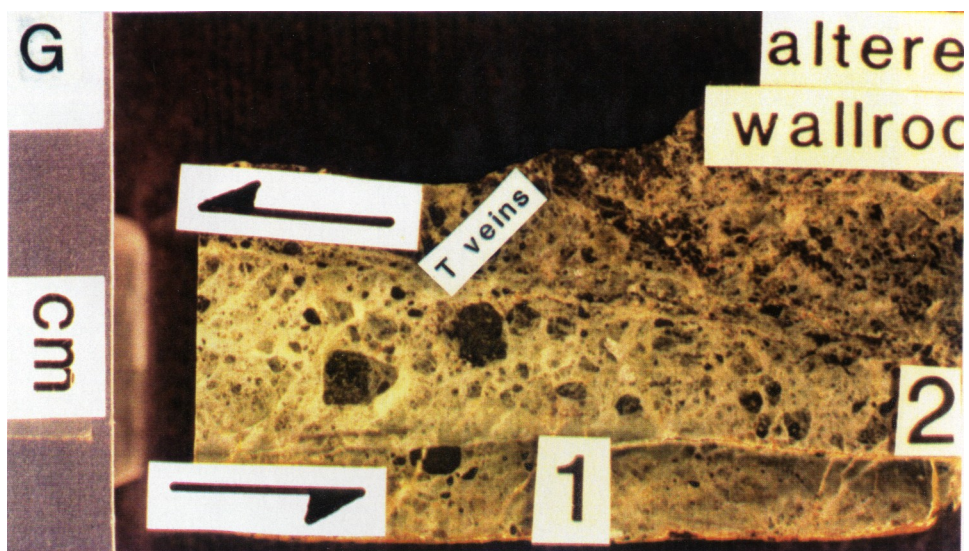


Figure 2 [g] Dike-parallel multiply-reactivated cataclasite (A-10, A-11, Table 3) with two generations (1 and 2) of prehnite + quartz cement. Slip sense determined in outcrop by offset dike margins and in hand sample by offset clasts, and secondary fractures including an en echelon array of prehnite + quartz (A-10, Table 3) filled extension (T) veins.



Figure 2 [h] Subvertical northern margin of highly fractionated dike (Figure 2a; A-34b in Table 1; event #9 in Figures 6a and 6b) which shows truncation of tilted dikes and hydrothermal veins (Figure 2f). Note the absence of veins in highly fractionated dike except in lower right where a pumpellyite + quartz and quartz + sulfide veins can be seen. Yellow and black colored 15 cm scale is in upper left quadrant of photo.

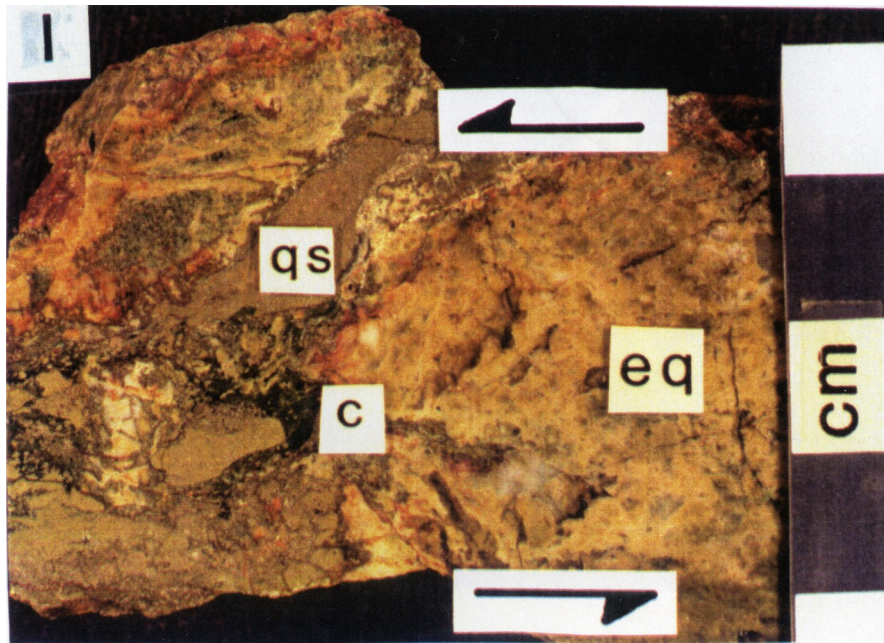


Figure 2 [i] Dike-parallel multiply-reactivated cataclasite with an early epidote + quartz (eq) cement (R-18, Table 3) as a porphyroblast in a quartz + sulfide (qs) \pm Fe-rich chlorite (c) cemented fault zone which juxtaposes the extrusive sequence on the upper sheeted dike complex. Not from the locality discussed in the text.

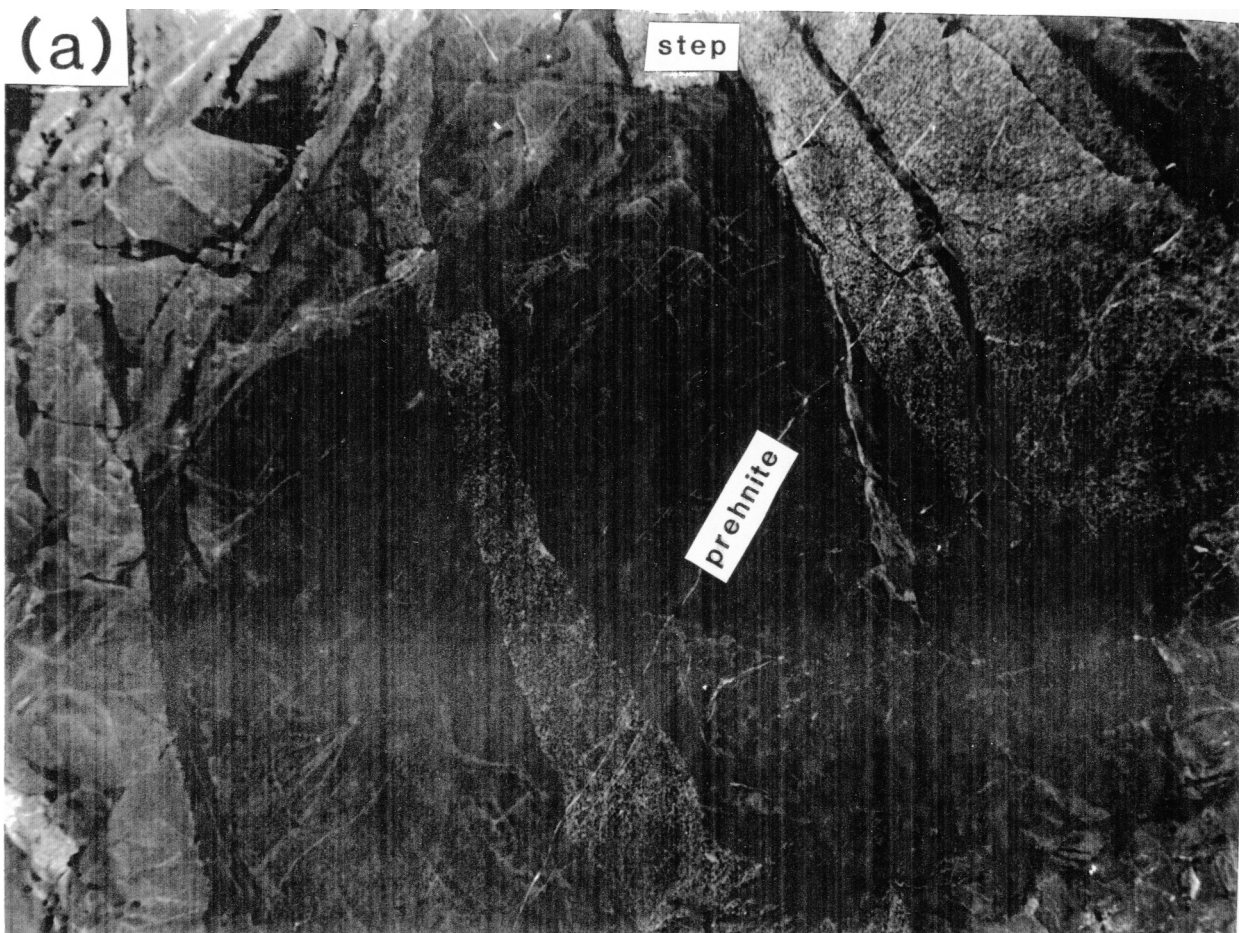


Figure 3 [a] Medium-grained amphibolite-grade isotropic gabbro intruded by several subparallel dikes with "stepped" margins. Positions of steps and veins on opposing dike margins indicate dike is a mode I (pure extension) fracture. Both gabbro and dike are crosscut by an anastomosing set of prehnite veins. 35 mm lense cap in upper right corner for scale.

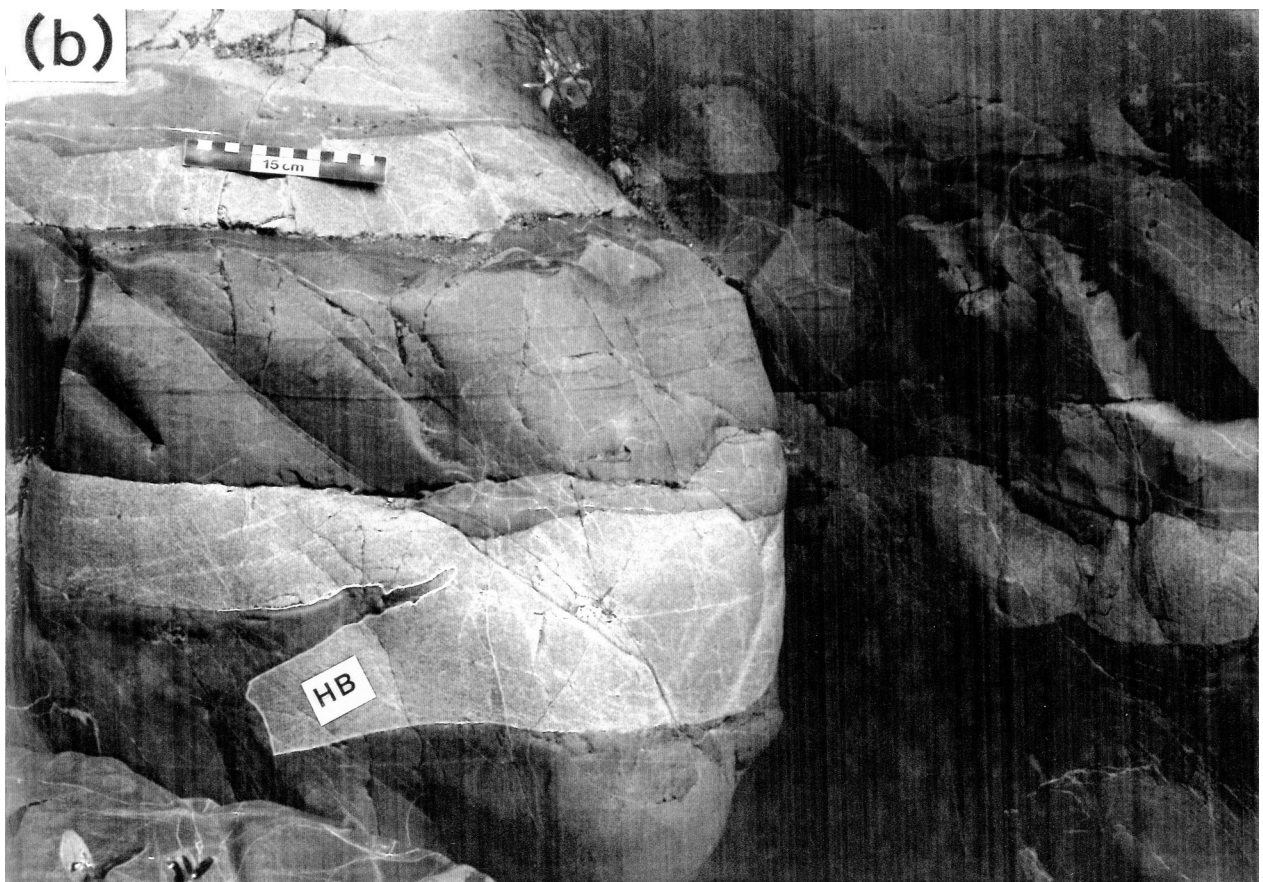


Figure 3 [b] Fine-grained gabbro intruded by two generations of dikes. Note dike margin "steps" and a "hanging bridge" (HB) of gabbro in lower left caused by linking of adjacent cracks during dike injection and dilation [*Nicholson and Pollard, 1985*].

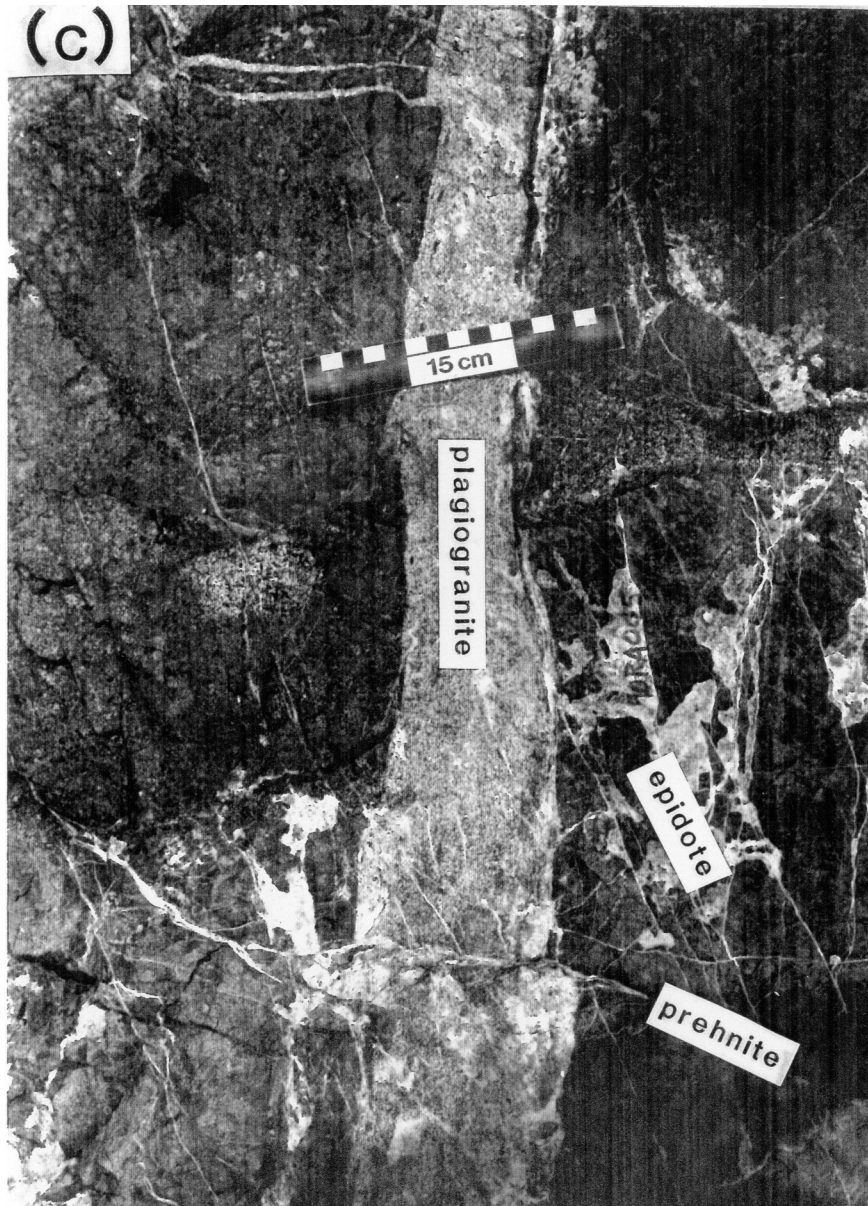


Figure 3 [c] Late stage plagiogranite dike intruded into a small-offset strike-slip fault (dike-perpendicular transfer fault). Host rock is an intrusive breccia composed of leucogabbro xenoliths in a mafic-rich gabbro matrix. Plagiogranite and wall rock are cross-cut by oblique epidote and prehnite extension veins which indicate latest fault motion is left-lateral.

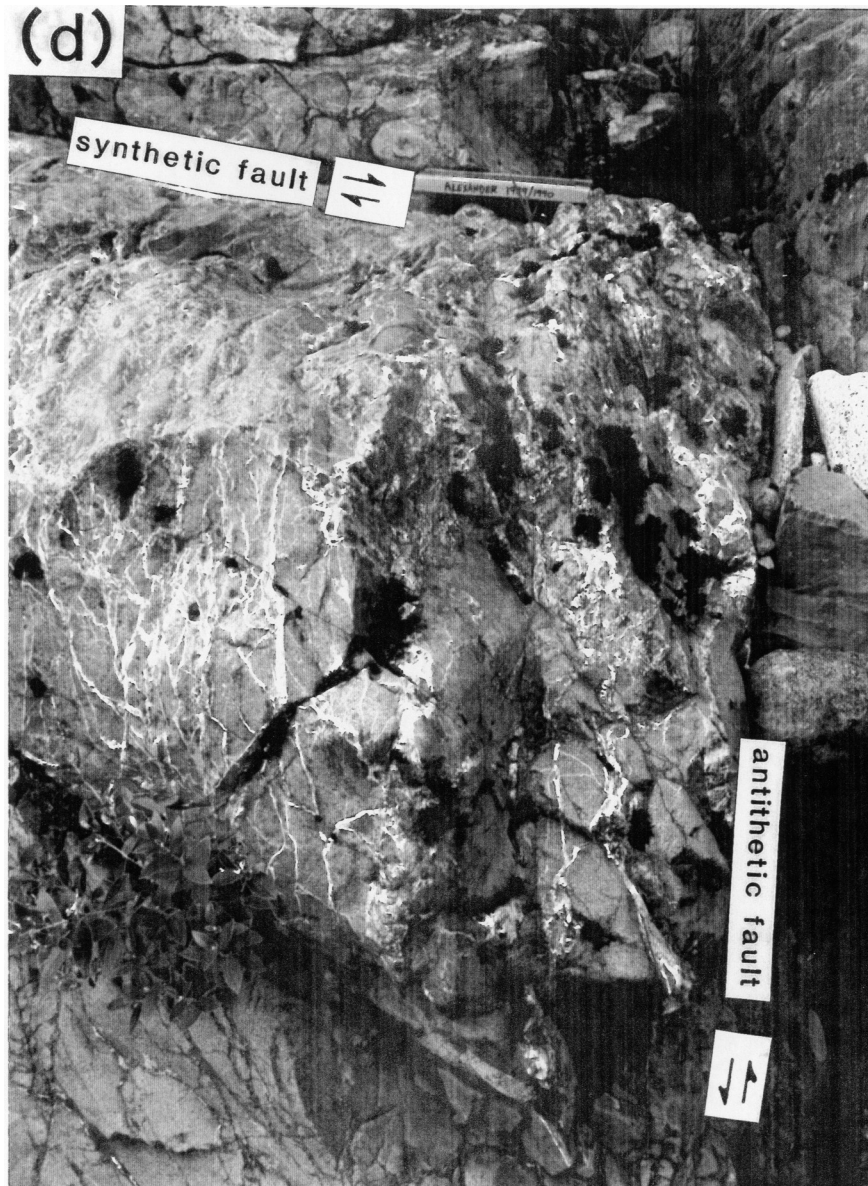


Figure 3 [d] Triangular-shaped zone of intense brecciation and hydrothermal veining at an oceanic fault intersection of a dike-parallel (synthetic) normal fault (parallel to plane of notebook) and a dike-perpendicular (antithetic) normal fault (subvertical on right) [see Figures 4 and 6a for location of fault intersection]. Note this fault block corner coincides with the extensional quadrant of the fault intersection.

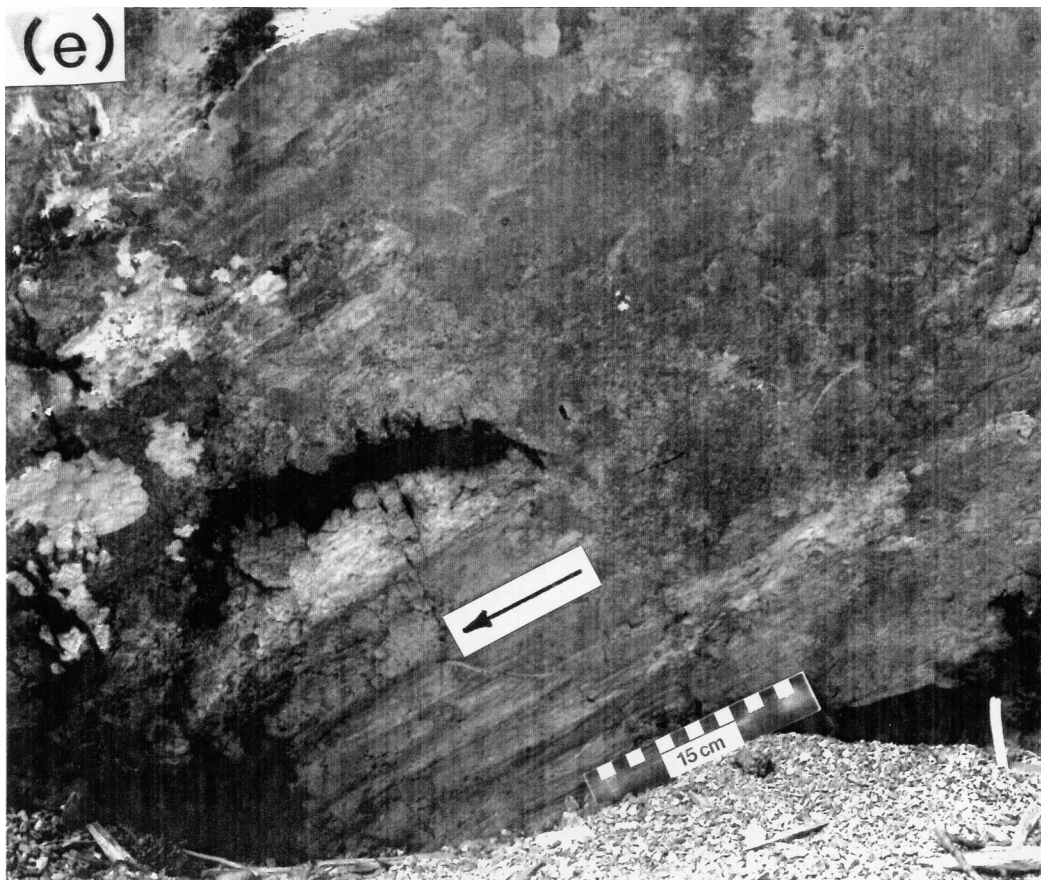


Figure 3 [e] Strike-slip (transfer) fault with oblique-slip (strike-slip > dip-slip) RM slickenstriae (arrow) indicating right-lateral slip sense. Fault zone locally has three different generations of cements of epidote + quartz, prehnite + quartz, and quartz + sulfide, each with different orientations of slickenstriae and shear sense.

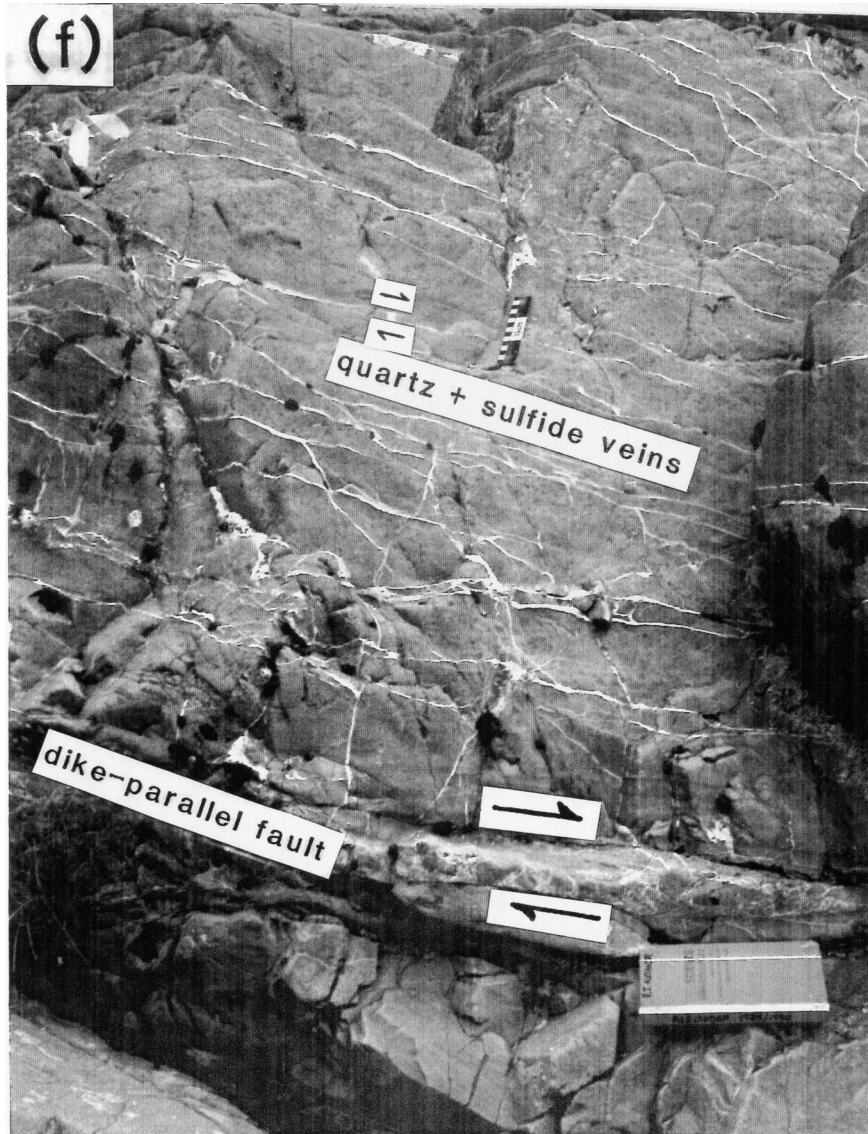


Figure 3 [f] Porphyritic dike with an orthogonal set of quartz + sulfide veins (A-13 in Table 3; event #13, Figures 6a and 6b) above a dike-parallel fault zone (see notebook). Veins show small extensional offsets (e.g., to the left of the scale in the middle of the photograph) which are compatible with slip sense on the dike-parallel normal fault zone.

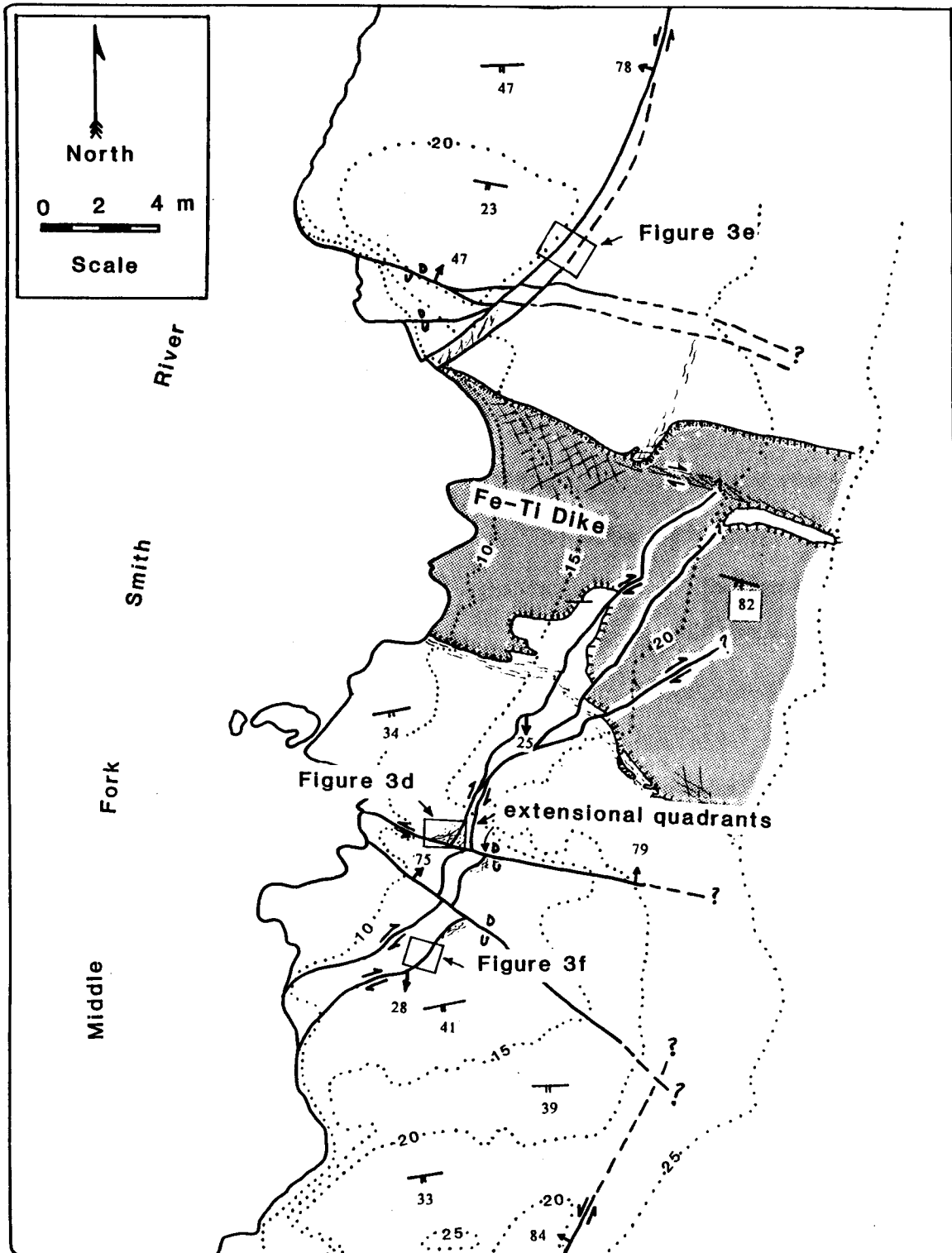


Figure 4 Geologic map of the water-polished outcrop along the east bank of the Middle Fork of the Smith River (Star in Figure 1). Bold lines are faults with dip direction and magnitude. Dotted lines are contours (5 ft. contour interval). Highly-fractionated dike (Fe-Ti dike, A-34b in Table 1) is shaded. Strike and dip of selected dike margins shown with double-ticks.

Outcrop Sketch at Big Bend

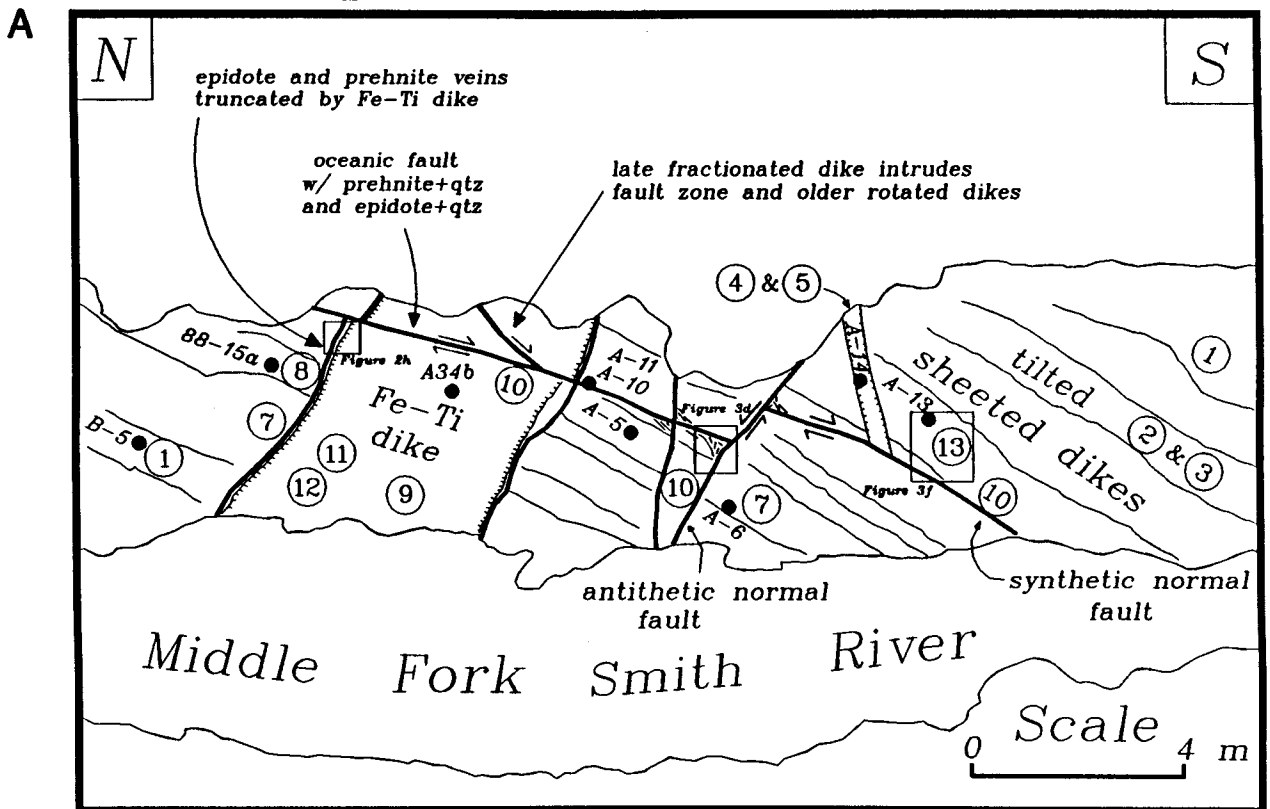


Figure 6 (A) Sketch cross section of the outcrop photograph in Figure 2a and corresponds to the map shown in Figure 4. Section is perpendicular to dikes. Solid circles show some of the sample localities in Tables 1 and 3.